ERDC/CHL TR-OX-X

Coastal and Hydraulics Laboratory

US Army Corps of Engineers®
Engineer Research and Development Center

Three Dimensional Shallow Water Adaptive Hydraulics (ADH-SW3): Hydrodynamic Verification and Validation

Gaurav Savant, R. Charlie Berger, Tate O. McAlpin and Corey J. Trahan

January 2014

Approved for public release; distribution is unlimited.

Three Dimensional Shallow Water Adaptive Hydraulics (ADH-SW3):

Hydrodynamic Verification and Validation

Gaurav Savant

Dynamic Solutions LLC
3909 Halls Ferry Rd.
Vicksburg, MS 39180

R. Charlie Berger, and Tate O. McAlpin

Coastal and Hydraulics Laboratory
U.S. Army Engineer Research and Development Center
3909 Halls Ferry Rd.
Vicksburg, MS 39180

Corey J. Trahan

Information Technology Laboratory
U.S. Army Engineer Research and Development Center
3909 Halls Ferry Rd.
Vicksburg, MS 39180

Final report

Approved for public release; distribution is unlimited [or a restricted statement]

Prepared for U.S. Army Corps of Engineers
Washington, DC 20314-1000

Under

Abstract: The U.S. Army Engineer Research and Development Center (ERDC) Coastal and Hydraulics Laboratory (CHL) has undertaken the development of the multi-module Adaptive Hydraulics (ADH) hydrodynamic, sediment, water quality and transport numerical hydrodynamic model. As a natural progression of this development process, verification of ADH was performed to known solutions for the basic physics contained in the model. This report documents verification and validation of the model performed by applying the model several analytic and flume experiments. These tests were designed to ensure that the SW3-ADH is solving the pertinent equations accurately.

DISCLAIMER: The contents of this report are not to be used for advertising, publication, or promotional purposes. Citation of trade names does not constitute an official endorsement or approval of the use of such commercial products. All product names and trademarks cited are the property of their respective owners. The findings of this report are not to be construed as an official Department of the Army position unless so designated by other authorized documents.

DESTROY THIS REPORT WHEN NO LONGER NEEDED. DO NOT RETURN IT TO THE ORIGINATOR.

Contents

Figures and Tables iv

Preface vi

Unit Conversion Factors vii

1 Introduction 9

Purpose of study 9

Verification and Validation Approach 10

Mesh Convergence and Adaption *10*

2 Testing 12

Mass Conservation 12

Response of Model to Tidal Propagation in a Closed Basin 16

Model Simulation of Free-Surface Seiching in a Closed Rectangular Basin 19

Model Response to Coriolis Forcing 23

Model Response to Wind Forcing 29

Flow around an Emergent Spur Dike: Test of Turbulence Closure 34

Propagation of Salinity Subsequent to a Lock Exchange 35

Baroclinic Transport in Reservoir 38

3 Summary and Conclusions 42

4 References 43

Report Documentation Page

Figures and Tables

Figures

Figure 1: Domain for Mass Conservation Test Case 12
Figure 2: Initial Displacement 13
Figure 3: Final Displacement 13
Figure 4: Model domain 16
Figure 5: Analytic Vs. Model generated results at X = 30m, Y = 15m 17
Figure 6: Error between Analytic and Model generated results at X = 30m, Y = 15m 17
Figure 7: Domain and Initial State for Free-Surface Seiche Problem 20
Figure 8: Displacement Results for Free-Surface Seiche Problem, 1 Mode 21
Figure 9: Displacement Results for Free-Surface Seiche Problem, 3 Modes 21
Figure 10: X Direction Velocity for Free-Surface Slosh, 1 Mode 22
Figure 11: Z Direction or Vertical Velocity for Free-Surface Slosh, 1 Mode 22
Figure 12: Test Domain for X-Direction Coriolis Forcing Test 24
Figure 13: Elevation variation along the test flume 24
Figure 14: Velocity Behavior for the X- Direction Coriolis test 24
Figure 15: Test Domain for Y-Direction Coriolis Forcing Test 25
Figure 16: Elevation variation along the test flume 27
Figure 17: Velocity Behavior for the Y- Direction Coriolis test 27
Figure 18: Test Domain for wind shear test cases. 29
Figure 19: Depths for the three flume orientations with a constant wind shear of 0.1 N/m^2 30
Figure 20: Velocity comparisons with a constant wind shear of 0.1 N/m^2 31
Figure 21: Velocity comparisons with a constant wind shear of 0.5 N/m^2 31
Figure 22: Domain for spur dike test. 34
Figure 23: Model Computed Recirculation Zone 34
Figure 24: Model computed recirculation zone in the vertical or 'z' axis. 35
Figure 25: Domain for lock exchange 36
Figure 26: Initial Constituent state for lock exchange 36
Figure 27: Base Case Constituent State at 16 seconds, red represents denser fluid. 36
Figure 28: Base Case (with Adaption) Constituent State at 16 seconds, red represents denser fluid. 37
Figure 29: Twice Refined Mesh Case Constituent State at 16 seconds, red represents denser fluid. 37
Figure 30: Plan View of GRH Test 38
Figure 31: Side View of GRH Test 39
Figure 32: Base Model Simulated Underflow State at 1140 sec (19 min). 39
Figure 33: Twice Refined Model Simulated Underflow State at 1080 sec (18 min) 40

Figure 34: Adapted Base Model Simulated Underflow State at 1080 sec (18 min).....40

Tables

Table 1: Model Behavior for Mass Conservation Tests, Number of Compute Nodes 1 15
Table 2: Model Behavior for mass Conservation Tests, Number of Compute Nodes 6Response of Model to a Periodic Forcing.....15
Table 3: Model Behavior for Periodic Forcing Tests, Number of Compute Nodes 1.....18
Table 4: Model Behavior for Periodic Forcing Tests, Number of Compute Nodes 32.....18
Table 5: Problem Parameters 19
Table 6: Model Parameters for Free-Surface Seiche Problem (all modes) 21
Table 7: Domain Discretization and Average Error, 1 mode 23
Table 8: Simulation Results for X Direction Coriolis Test Case, 96 Compute Nodes.....26
Table 9: Simulation Results for Y Direction Coriolis Test Case, 96 Compute Nodes 28
Table 10: Comparison of the AdH model results to the analytical solution for all simulated scenarios. 33
Table 11: Simulation Results for Flow around a Spur Dike Test Case, 96 Compute Nodes.....35
Table 12: Simulation Parameters for Lock Exchange Test Case 37
Table 13: Simulation Results for Lock Exchange Test Case, 32 Compute Nodes.....38
Table 14: Simulation Results for Lock Exchange Test Case, 96 Compute Nodes.....38
Table 15: Simulation Parameters for GRH Test Case.....39
Table 16: Simulation Results for GRH Test Meshes.....41

Preface

This report represents the findings of the ADH-SW3 verification and validation efforts. ADH-Sw3 demonstrates the capability to accurately and adequately represent hydrodynamics as well as associated baroclinic transport phenomenon of importance in a stratified environment associated with navigation channels, reservoirs etc.

This investigation was conducted from January 2012 through December 2013 at the U.S. Army Engineer Research and Development Center (ERDC) by Dr. Gaurav Savant, Mr. Tate O. McAlpin and Dr. R.C. Berger of the Coastal and Hydraulics Laboratory (CHL). Funding was provided by the Flood and Coastal Research Program of the USACE.

The work was performed under the general direction of Jose Sanchez, Director, CHL, Dr. Ty V. Wamsley, Chief, Flood and Storm Protection Division, and Dr. Robert McAdory, Chief, Estuarine Engineering Branch, CHL.

At the time of publication of this report, Dr. Jeffery P. Holland was Director of ERDC, and COL Kevin J. Wilson was Commander and Executive Director.

Unit Conversion Factors

Multiply	By	To Obtain
cubic feet	0.02831685	cubic meters
cubic yards	0.7645549	cubic meters
degrees (angle)	0.01745329	radians
feet	0.3048	meters
knots	0.5144444	meters per second
microns	1.0 E-06	meters
miles (nautical)	1,852	meters
miles (U.S. statute)	1,609.347	meters
miles per hour	0.44704	meters per second
pounds (force)	4.448222	newtons
slugs	14.59390	kilograms
square feet	0.09290304	square meters
square miles	2.589998 E+06	square meters
square yards	0.8361274	square meters
yards	0.9144	meters

1 Introduction

The U.S. Army Corps of Engineers (USACE), through the U.S. Army Engineer Research and Development Center, has developed a robust multi-dimensional mass conservative finite element hydrodynamic and constituent transport numerical code Adaptive Hydraulics (ADH).

ADH is a modular code with the capability to simulate varied physics such as saturated and unsaturated groundwater flow, Navier-Stokes flow, overland flow as well as two-dimensional shallow water flow. As part of the natural progression of ADH capability, a three dimensional shallow water module (ADH-SW3) has now been developed and is currently undergoing testing for robustness, accuracy and sufficiency of model numerics.

ADH-SW3 represents a generational improvement in USACE capability to model riverine, estuarine and reservoir physics due to the following:

1. Linear triangles based meshing allows for accurate and adequate representation of bathymetry,

2. Vertical meshing that is neither Sigma or Z-grid based and hence, is not encumbered by the drawbacks of either,

3. Run time adaption in the horizontal and vertical allows for accurate representation of hydrodynamics as well as transport,

4. Conservation of fluid and constituent mass,

5. Easy transition from the two-dimensional realm to the three-dimensional.

Purpose of study

The objectives of this study were to evaluate the capability of ADH-SW3 to accurately and adequately replicate hydrodynamics and transport through application to a suite of analytic and experimental field studies.

Verification and Validation Approach

The approach utilized in this study was designed to replicate the order in which the code was created. The tests performed in order were:

A) Verification Tests:
These are tests which are performed to ascertain whether the code is solving the correct equations accurately and involve the solution of analytic problems whose solutions are known. A verification test is successfully completed if the numerical model can reproduce the analytic solution without any modification to the model parameters from those specified in the analytic problem.

ADH-SW3 was subjected to the following verification tests:

- Basic tests to ensure that the model is conserving fluid and constituent mass,
- Response of model to periodic forcing,
- Response of model to free-surface Seiche in closed frictionless basin,
- Model response to coriolis forcing, and
- Model response to wind forcing

B) Validation Tests:
These are tests performed to exercise the code through application to flume studies and/or real world problems. A validation test involves application of the code to the problem where physical parameters such as roughness are known. Modification of model parameters is usually allowed within scientifically acceptable ranges. If observed values are known for the problem no modification of parameters is allowed.

ADH-SW3 was subjected to the following validation tests:

- Flow around a spur dike: Test of turbulence closure models,
- Propagation of salinity generated density current subsequent to a lock exchange, and
- Propagation of temperature generated density current within a reservoir.

Mesh Convergence and Adaption

A basic tenet of numerical modeling is that as the mesh and time step are refined a model should converge to the underlying equation that are being solved. In our comparisons to the solutions, either analytic or experimental, we run three different meshes. The first mesh is the “base” mesh generated to adequately represent the problem domain, and the second mesh has twice the resolution of the “base” mesh in the horizontal and the vertical. The second mesh is considered to be a high resolution mesh and the results should be converged. ADH-SW3 is an adaptive mesh model and so mesh is added automati-

cally (and in some cases removed, but the resolution never goes below the base resolution). This capability allows the model to add resolution when and where needed. Within this verification and validation exercise we will demonstrate that adaption is working to give results that are converged with a lesser computational effort. This computational effort roughly correlates with the number of nodes in the mesh.

2 Testing

Mass Conservation

Mass conservation is a basic tenet of numerical modeling and numerical codes utilizing the conservative form of the shallow water equations must conserve fluid as well as constituent mass. SW3-ADH is written to be mass conservative and hence the first test performed on the code was a mass conservation test.

The domain for this test consisted of a cuboid flume 40,000 m (length), 8,000 m (width) and 12 m (depth). This domain is represented in figure 1. The water surface was initially perturbed by 0.25 m at the left hand wall of the flume and displacement at the right hand wall was set at -0.25 (figure 2)..

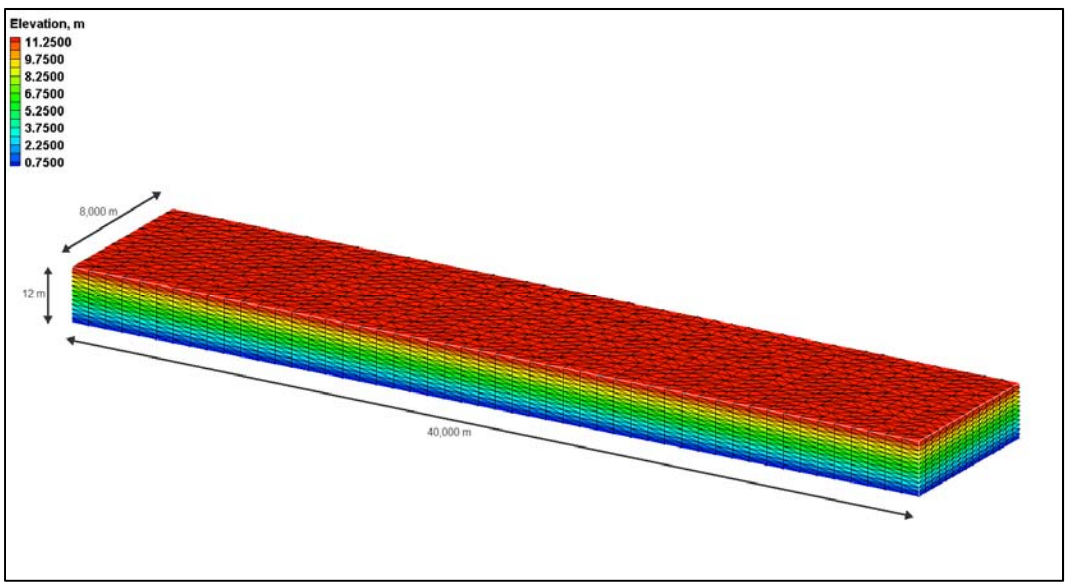

Figure 1: Domain for Mass Conservation Test Case

This configuration provides an initial volume of fluid in the basin of 3,840,000,000 cubic meters. The model is allowed to slosh for 1 day and the fluid volume recalculated. In the absence of external inflows and coding errors a conservative model must have the same volume of fluid at 86400 seconds as was present at 0.0 seconds

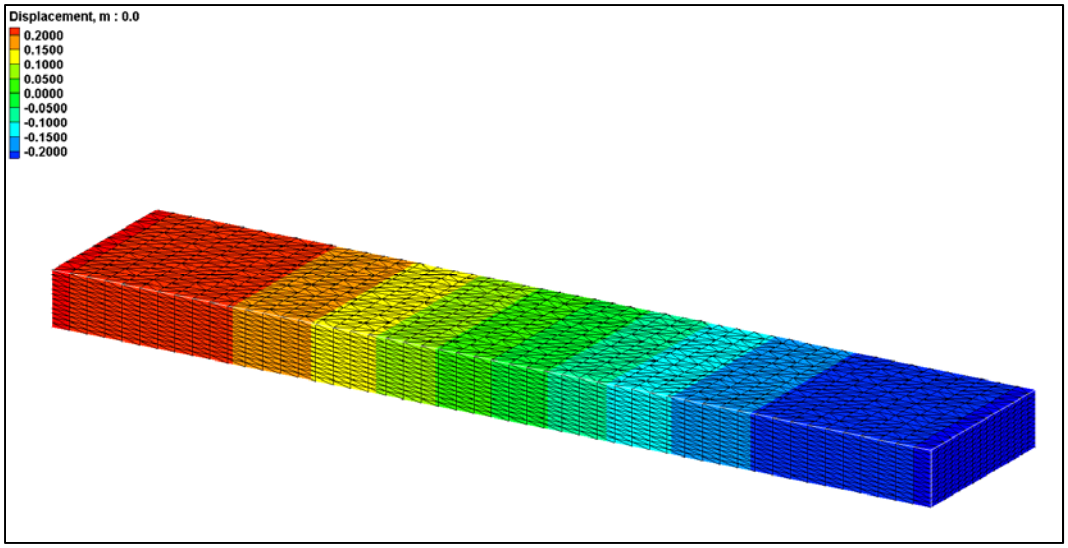

Figure 2: Initial Displacement

Figure 3, illustrates the final model state (in terms of displacement) at 86400 seconds. As would be expected for a conservative model the displacement is at 0.0 m (~ 0.0000001 m). This provides a fluid volume of 3,840,000,000 cubic meters, the same as the fluid volume at 0 seconds.

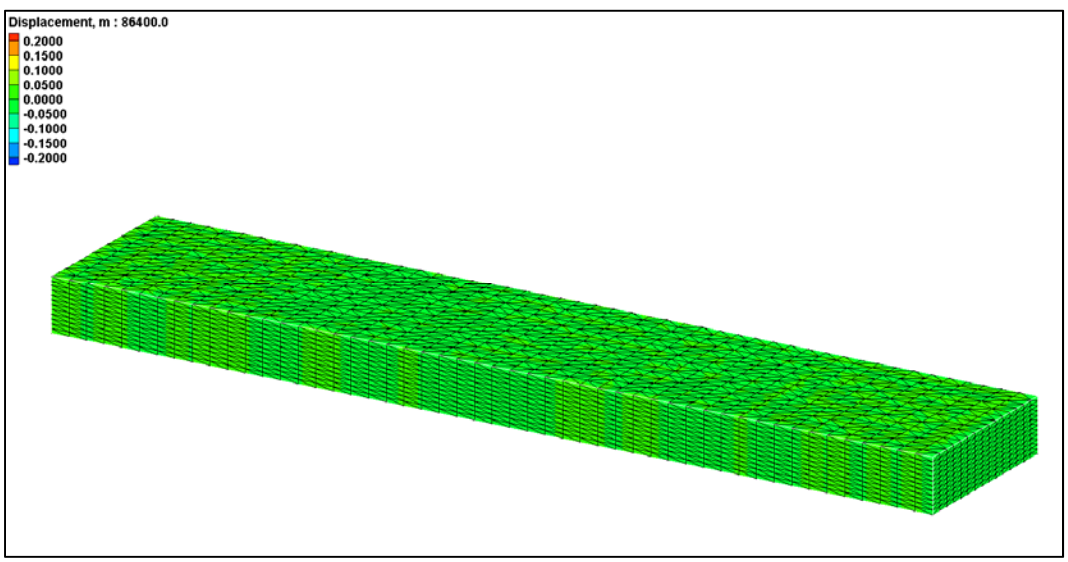

Figure 3: Final Displacement

To test constituent mass conservation, the concentration of a generic constituent was specified as 0.035 kg/m^3 for a total constituent mass of 134,400,000 kg. At the end of simulation the total mass was conserved, though there were local variations in the exact value of constituent concentration, these deviations were in general less than 0.002 kg/m^3. Tables 1 and 2 present the results of the mesh resolution test performed to ascertain the effects of resolution on fluid and constituent mass conservation and the effect of number of processors used respectively. As expected the higher resolution mesh provides a very

slight improvement in the results and the code provides essentially the same results for both 1 and 6 processors. It must be emphasized that both mesh resolutions conserve fluid and constituent mass to at least the non-linear tolerance specified.

Horizontal Node Spacing (m)	Number of Vertical Layers	Total/Max Number of Nodes	Model Water Level (m)	Theoretical Water Level (m)	Water Level Error (m)	Model Concentration (kg/m^3)	Theoretical Concentration (kg/m^3)	Concentration Error (kg/m^3)
800x533.33	12	10608	-4.3391e-009	0.0000	-4.3391e-009	0.034998	0.035	-2.0×10^{-6}
400x266.67	24	78275	-3.6106e-009	0.0000	-3.6106e-009	0.034999	0.035	-1.0×10^{-6}
800x533.33, Adaption	12, Adaption	29358	-3.5426 e-009	0.0000	-3.5426e-009	0.034999	0.035	-1.0×10^{-6}

Table 1: Model Behavior for Mass Conservation Tests, Number of Compute Nodes 1

Horizontal Node Spacing (m)	Number of Vertical Layers	Total/Max Number of Nodes	Model Water Level (m)	Theoretical Water Level (m)	Water Level Error (m)	Model Concentration (kg/m^3)	Theoretical Concentration (kg/m^3)	Concentration Error (kg/m^3)
800x533.33	12	10608	-4.3256e-009	0.0000	-4.3256e-009	0.034999	0.035	-1.0×10^{-6}
400x266.67	24	78275	-3.5245e-009	0.0000	-3.5245e-009	0.034999	0.035	-1.0×10^{-6}
800x533.33, Adaption	12, Adaption	29355	-3.5409 e-009	0.0000	-3.5409e-009	0.034999	0.035	-1.0×10^{-6}

Table 2: Model Behavior for mass Conservation Tests, Number of Compute Nodes 6Response of Model to a Periodic Forcing

Response of Model to Tidal Propagation in a Closed Basin

This test was designed to test the accuracy of the time integration scheme implemented in representing the propagation of an undamped sine wave in a rectangular channel**.** The basin is open at one end, enclosed on all others, and the "free slip" velocity condition is assumed on the internal walls. The model domain is represented in figure 4. The sine wave applied at the boundary is written as:

$$h = (1.0)Sin(t)$$

Where, h is the water surface displacement, and t is the time.

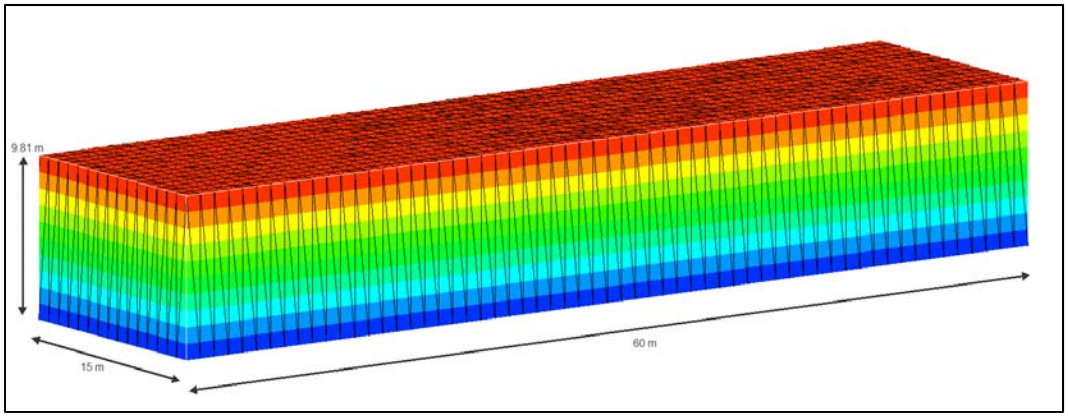

Figure 4: Model domain

The physical constants are acceleration due to gravity 'g' = 9.81m/s^2 and initial depth 'H' = 9.81 m.

The analytic spatially and time varying solution of this wave is provided in *Taylor and Davis (1975)* and is:

$$h = (1.0)Sin(t - x/9.81)$$

Where, x is the longitudinal distance from the open boundary. Figure 5, provides a comparison of the analytic solution and the model generated results. The error between the analytic and the model solution is provided in figure 6.

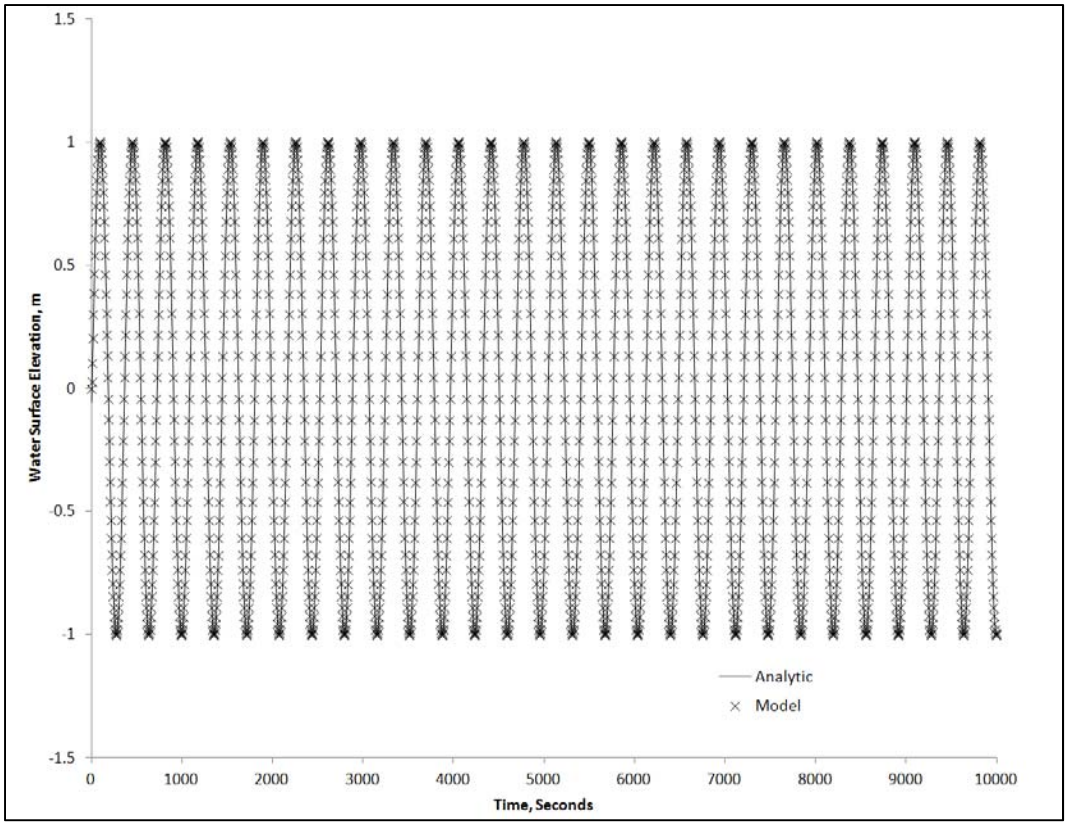

Figure 5: Analytic Vs. Model generated results at X = 30m, Y = 15m

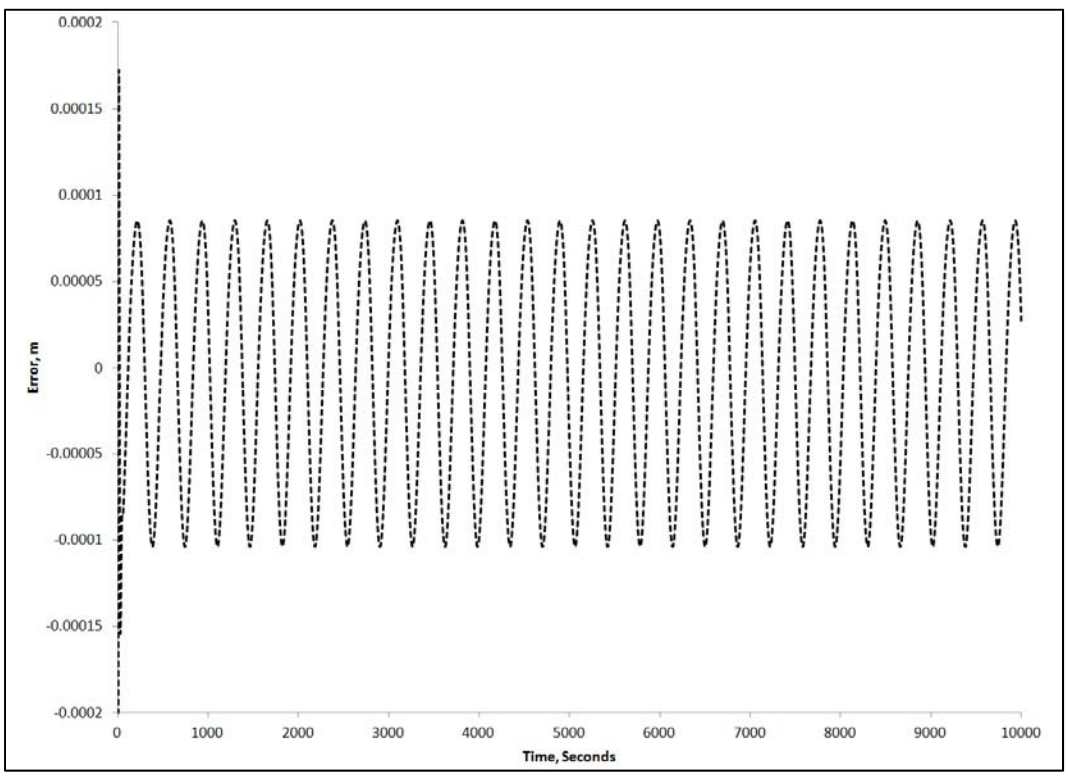

Figure 6: Error between Analytic and Model generated results at X = 30m, Y = 15m

Horizontal Node Spacing (m)	Number of Vertical Layers	Total/Max Number of Nodes	Average Water Level Error (m)
1x1	1	1952	-2.6117E-04
0.5x0.5	2	11253	2.5E-04
0.5x0.5	12	48763	2.8005E-04
1x1, adaption	1	2753	-2.5461E-04

Table 3: Model Behavior for Periodic Forcing Tests, Number of Compute Nodes 1

Horizontal Node Spacing (m)	Number of Vertical Layers	Total/Max Number of Nodes	Average Water Level Error (m)
1x1	1	1952	-5.24E-04
0.5x0.5	2	11253	3.2148-04
0.5x0.5	12	48763	1.7513-04
1x1, adaption	1	3259	-4.175-04

Table 4: Model Behavior for Periodic Forcing Tests, Number of Compute Nodes 32

Model Simulation of Free-Surface Seiching in a Closed Rectangular Basin

In a frictionless closed basin the oscillation generated due to an initial perturbation in the free-surface is a result of interaction between inertia and gravity. The analytic solution is easily obtained and is represented as:

$$\eta = \frac{H}{2}\cos(kx)\cos(\sigma t)$$
$$u = \frac{H}{2}\sigma\frac{\cosh(k(h+z))}{\sinh(kh)}\sin(kx)\sin(\sigma t)$$
$$w = -\frac{H}{2}\sigma\frac{\sinh(k(h+z))}{\sinh(kh)}\cos(kx)\sin(\sigma t)$$

Where, η is the water surface elevation, σ is frequency of the wave, u is the horizontal x-direction velocity, w is the vertical velocity, h is the average fluid depth, z is the vertical ordinate, H is the peak to peak wave amplitude, x is the horizontal distance, t is the time since initialization of the perturbation and k is the wave number. The y-direction velocity for a free-surface Seiche in a frictionless closed basin is '0' at all times for all locations within the domain.

The setup of this problem investigates accuracy of the temporal acceleration term implementation.

The basic parameters of this problem are presented in table 5.

Peak to Peak Amplitude	0.5m
Mean Water Depth	100m
Wave Mode	1 and 3
Length of Basin	120,000m
Wavelength	240000m and 80000m

Table 5: Problem Parameters

For a mode of 'm' the length of the domain to generate a standing wave is determined as:

$$L = \frac{2l}{m}$$

Where, L is the wavelength, l is length of the domain and m is the wave mode.

Under the parameters presented the wave characteristics are of a standing wave and the model should reproduce this behavior. This is a linear problem and ADH-SW3 is attempting to solve it utilizing a system of non-linear equations therefore we expect the model to deviate from the analytic solution for large perturbations.

Figure 7 presents the initial domain state for the problem with 3 modes (red represents 0.25m and blue represents -0.25m).

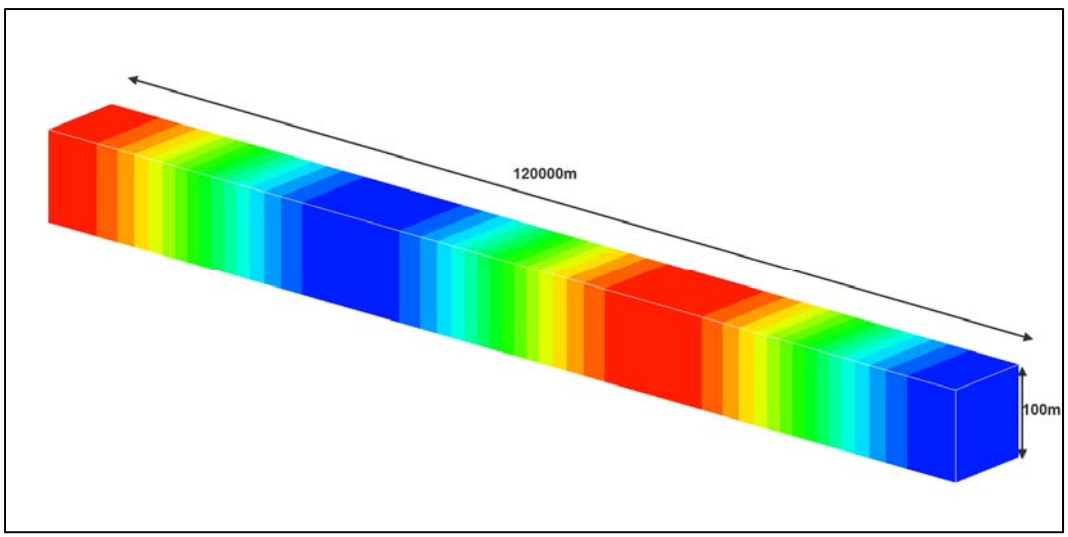

Figure 7: Domain and Initial State for Free-Surface Seiche Problem

Model parameters for this test are presented in table 6. Please note that all results presented are from the test case where mesh adaption was turned on.

Parameter	Base Mesh	Adapted Mesh	Twice Refined Mesh
Background Kinematic Eddy Viscosity	0.00	0.00	0.00
Manning's "n"	0.0	0.0	0.0
Turbulence Model	OFF	OFF	OFF

Table 6: Model Parameters for Free-Surface Seiche Problem (all modes)

Figures 8 and 9 presents the results from the model simulation (1 and 3 modes respectively) with the adapted mesh at a point in the domain located at x=81000 m from left end of the mesh.

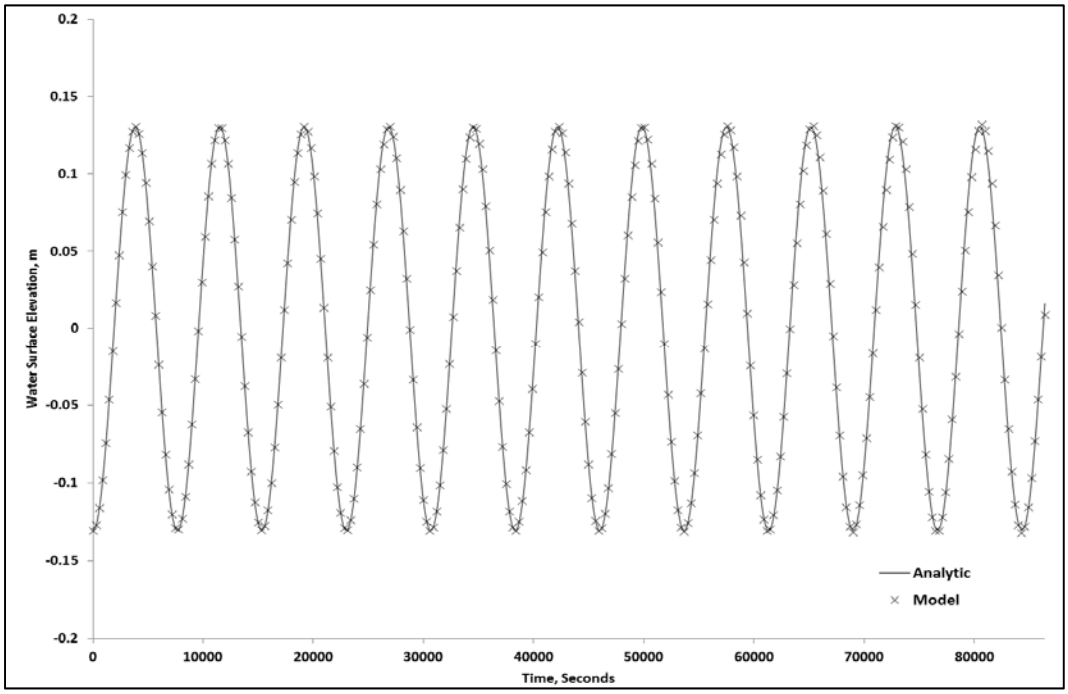

Figure 8: Displacement Results for Free-Surface Seiche Problem, 1 Mode

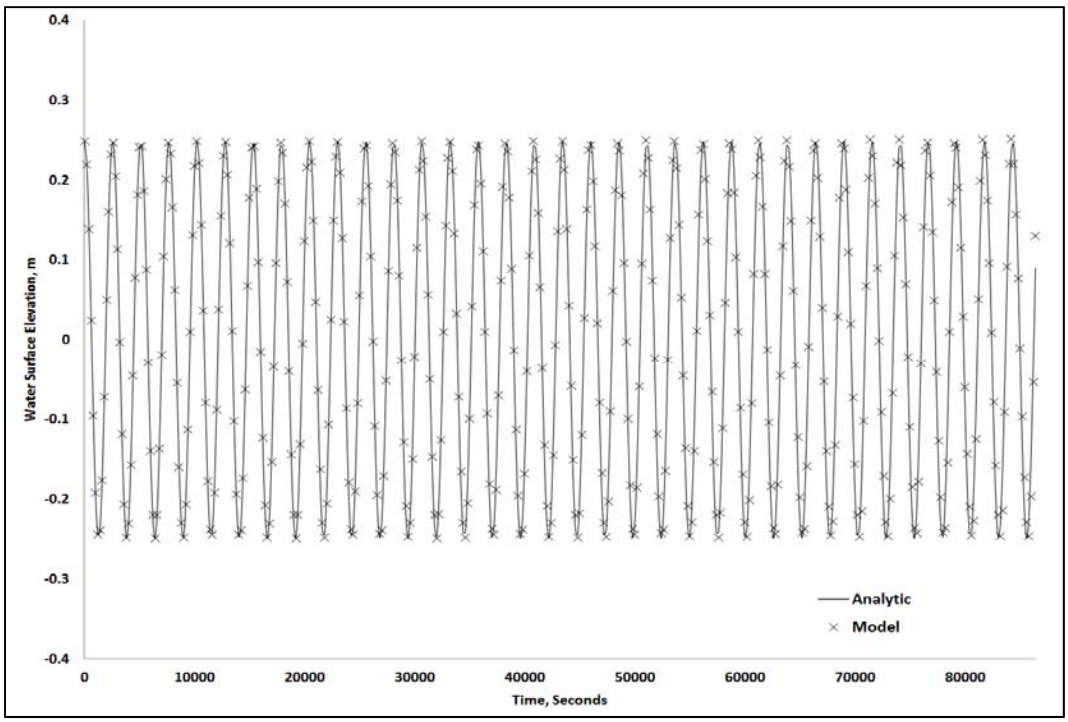

Figure 9: Displacement Results for Free-Surface Seiche Problem, 3 Modes

Figure 10 and 11 show the comparison between the X-direction and vertical velocities for the 1 mode test case.

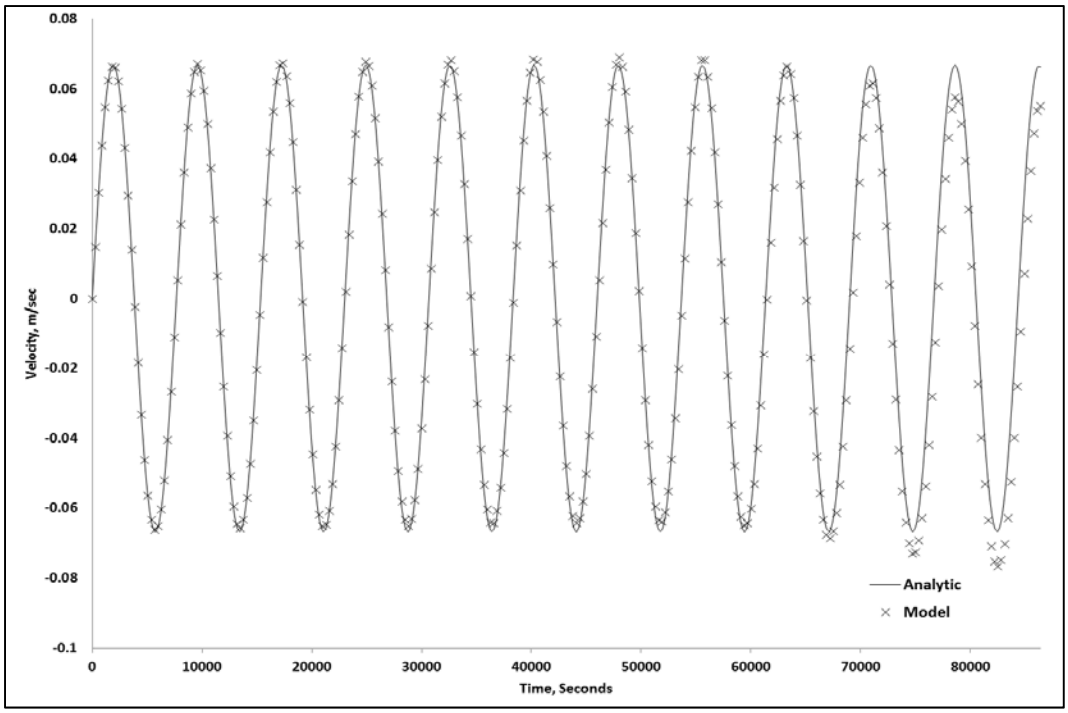

Figure 10: X Direction Velocity for Free-Surface Slosh, 1 Mode

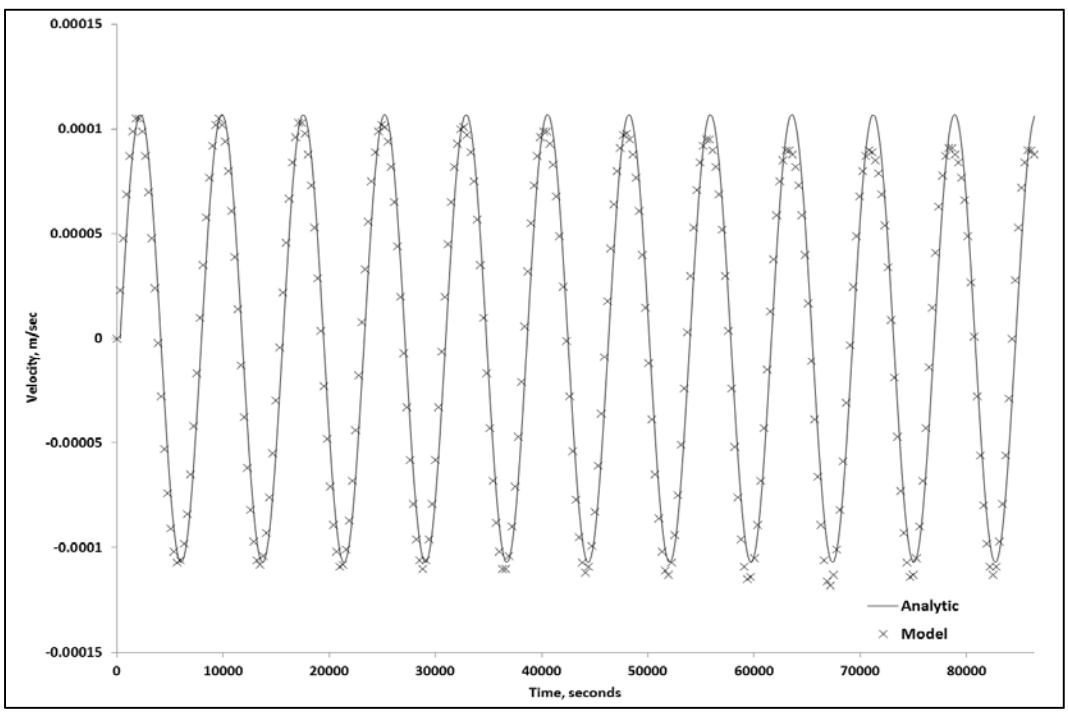

Figure 11: Z Direction or Vertical Velocity for Free-Surface Slosh, 1 Mode

Horizontal Node Spacing, m	Number of Vertical Layers	Time step, sec	Average Error, (Analytic – Model)		
			Water Surface, m	X – Velocity, m/sec	W-Velocity, m/sec
6000x6000	1	50	-0.00014	0.003	2E-6
3000x3000	2	50	-0.00001	0.002	1.2E-6
6000x6000(adapted)	1	50 (adapted)	-0.00003	0.002	1.4E-6

Table 7: Domain Discretization and Average Error, 1 mode

Model Response to Coriolis Forcing

A simplified system was set up to test the water surface slope variation due to coriolis in the x direction and the y direction. The flume for testing the x-direction test has a flat bottom and is dimensioned as shown in figure 12.

In the x direction, the y velocity is zero and the change in the u velocity with respect to x is zero assuming uniform flow, therefore the x equation simplifies to zero and the y equation reduces to

$$\frac{\delta h}{\delta y} = -\frac{2\omega \sin\theta \ u}{g}$$

Using the known parameters and latitude of 45◦, the water surface slope should be -2.0988e-6 m/m. The model simulation provides a slope of -2.154e-6 m/m (figure 13). The velocity direction indicates a curvature toward the right (figure 14) which is supported by the Coriolis theory.

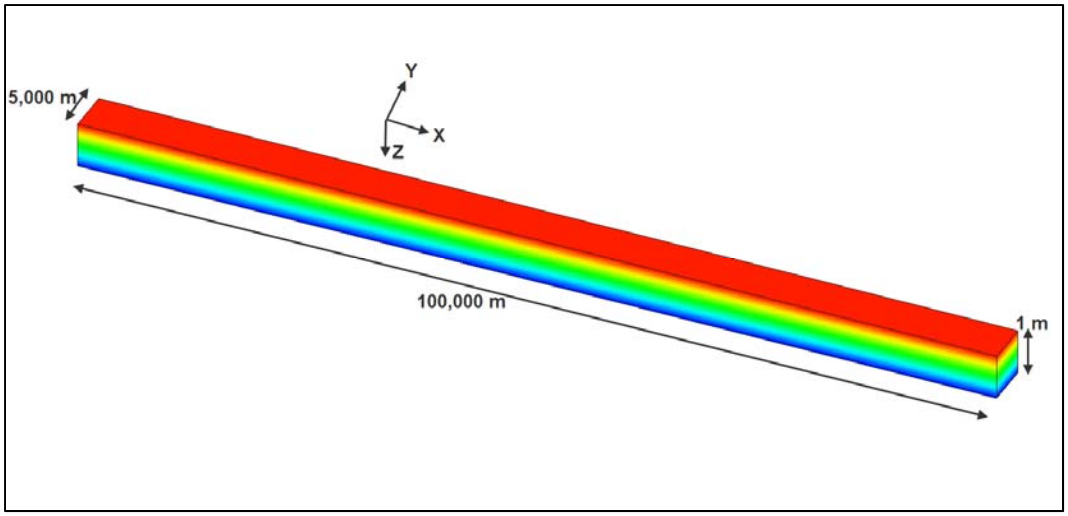

Figure 12: Test Domain for X-Direction Coriolis Forcing Test

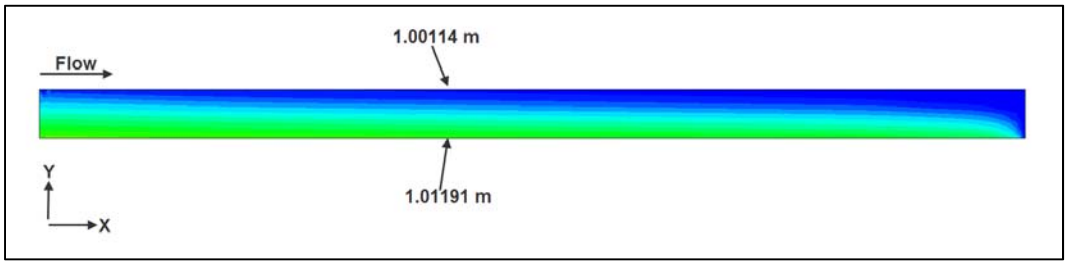

Figure 13: Elevation variation along the test flume

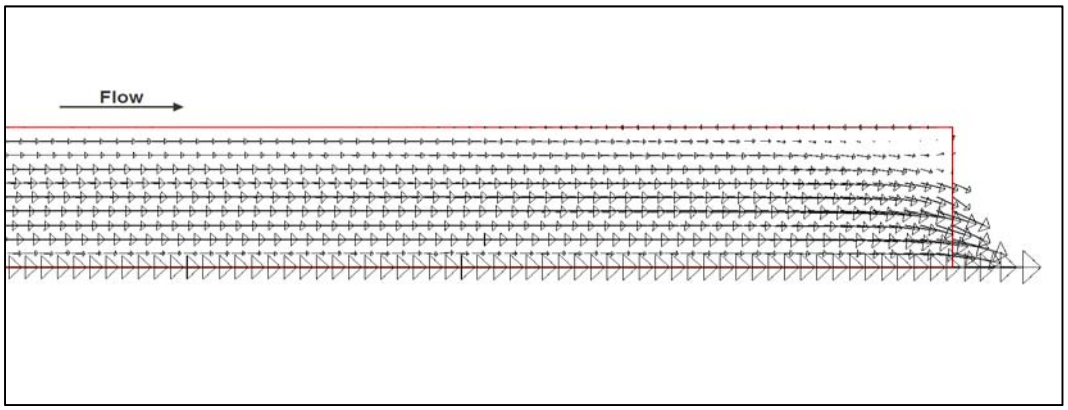

Figure 14: Velocity Behavior for the X- Direction Coriolis test

In the y direction, the u velocity is zero and the change in the v velocity with respect to y is zero assuming uniform flow, therefore the y equation simplifies to zero and the x equation reduces to

$$\frac{\delta h}{\delta x} = -\frac{2\omega \sin\theta \ v}{g}$$

Figure 15 illustrates the domain for this test (the image is rotated for ease of illustration).

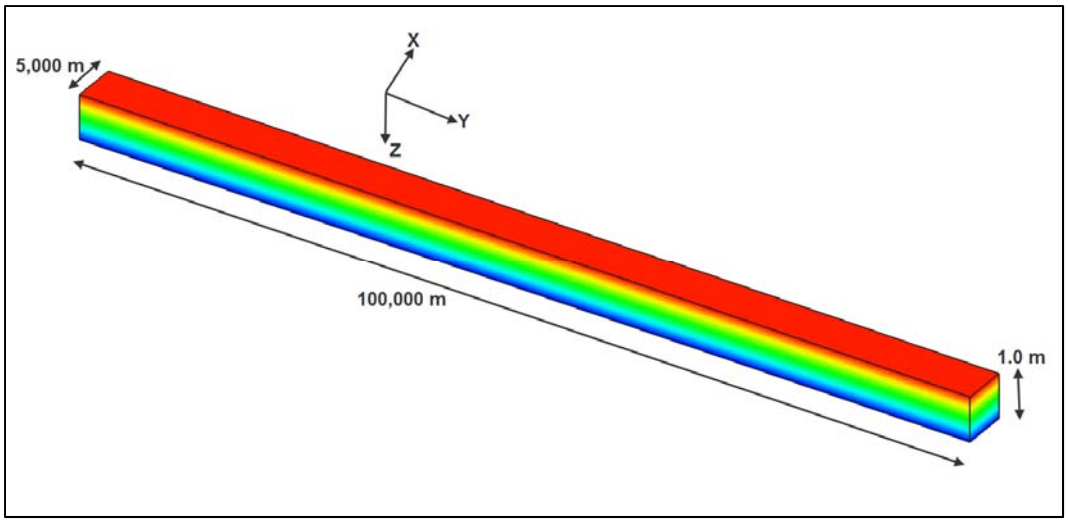

Figure 15: Test Domain for Y-Direction Coriolis Forcing Test

Using the known parameters, the water surface slope, again, should be -2.0988e-6 m/m. The model simulation provides a slope of -2.0000e-6 m/m (figure 16). The velocity direction (figure 17) indicates a curvature toward the right which is again supported by the Coriolis theory.

Horizontal Node Spacing (m)	Number of Vertical Layers	Total/Max Number of Nodes	Slope (m/m)	Analytic Slope (m/m)	Slope Error
500x500	5	13266	-2.154e-6	-2.0988e-6	5.58e-8
250x250	8	92631	-2.118e-6	-2.0988e-6	1.92e-8
500x500 (adaption)	5	15894	-2.121e-6	-2.0988e-6	2.22e-8

Table 8: Simulation Results for X Direction Coriolis Test Case, 96 Compute Nodes

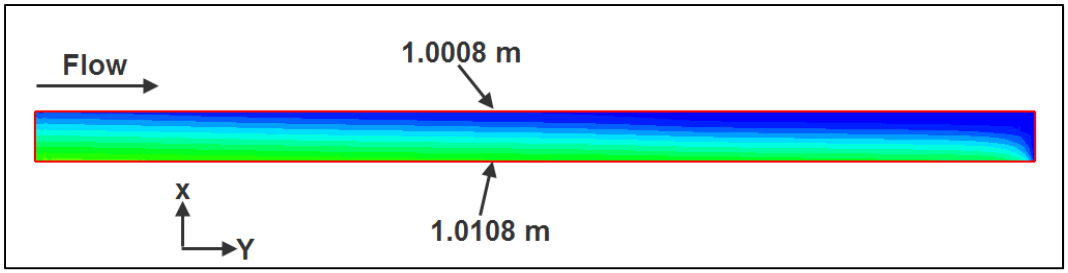

Figure 16: Elevation variation along the test flume

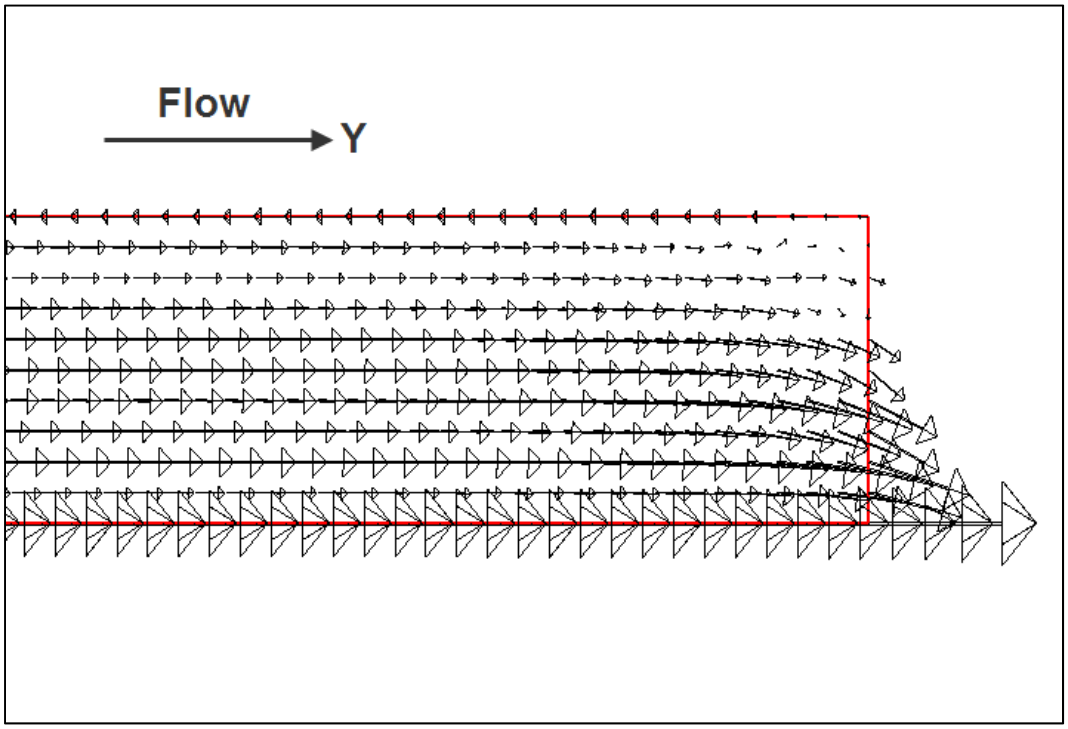

Figure 17: Velocity Behavior for the Y- Direction Coriolis test

Horizontal Node Spacing (m)	Number of Vertical Layers	Total/Max Number of Nodes	Slope (m/m)	Analytic Slope (m/m)	Slope Error
500x500	5	13266	-2.000e-6	-2.0988e-6	9.88e-8
250x250	8	92631	-2.058e-6	-2.0988e-6	4.08e-8
500x500 (adaption)	5	15895	-2.025e-6	-2.0988e-6	7.38e-8

Table 9: Simulation Results for Y Direction Coriolis Test Case, 96 Compute Nodes

Model Response to Wind Forcing

A simplified system was set up to test the water surface slope and three-dimensional return current generated by applying a constant wind shear to the water surface. The flume shown in Figure 13 had a flat bottom with an initial 40 meter depth. The test simulations had the flume oriented in three different directions (the x-direction, y-direction, and at a 45 degree angle to the x direction) to properly test the wind application in both the x and y directions independently and then concurrently for the 45 degree configuration. All wind shears were applied such that the shear direction was oriented in the same direction as the flume.

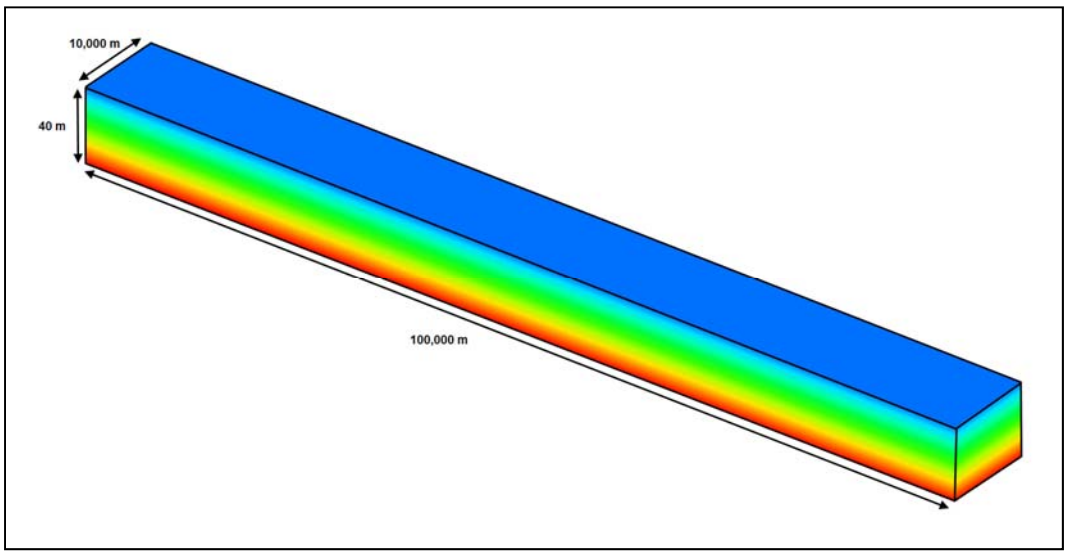

Figure 18: Test Domain for wind shear test cases.

The simulations also investigated the relative error associated with changes in the magnitude of the wind shears (simulated wind shears of 0.1 N/m^2 and 0.5 N/m^2) along with the impact of varying both the horizontal resolution (500 meters and 1,000 meters) and vertical mesh resolutions (6, 8, 12 and 20 vertical layers).

The analytical water surface elevation was calculated using

$$\Delta h = \frac{\tau L}{\rho g h}$$

where τ is the applied wind shear ($\tau = 0.1\ \frac{N}{m^2}$ and $\tau = 0.5\ \frac{N}{m^2}$), L is the length of the flume ($L = 100{,}000\ m$), ρ is the density of water ($\rho = 1{,}000\ \frac{kg}{m^3}$), g is gravity ($g = 9.817\ \frac{m}{s^2}$), h is the flume depth ($h = 40\ m$), and Δh is the change in water level along the length of the flume (*Wang, et al, 2009*).

The analytical solution for the vertical velocity profile is

$$u = \frac{1}{6K_v} gSh^2[3(\delta - 1)^2 - 1] + \frac{\tau h}{2\rho K_v}(2\delta - 1)$$

where K_v is the constant vertical eddy viscosity ($K_v = 0.03\ \frac{m^2}{s}$), S is the water level slope, δ is the non-dimensional or normalized vertical coordinate measure from the bed ($\delta = 0$) to the water surface ($\delta = 1$), and u is the velocity for the specified depth (*Wang, et al, 2009*).

The AdH water surface elevation solutions for all three flume orientations are shown in Figure 16 for the $\tau = 0.1\ \frac{N}{m^2}$ wind shear.

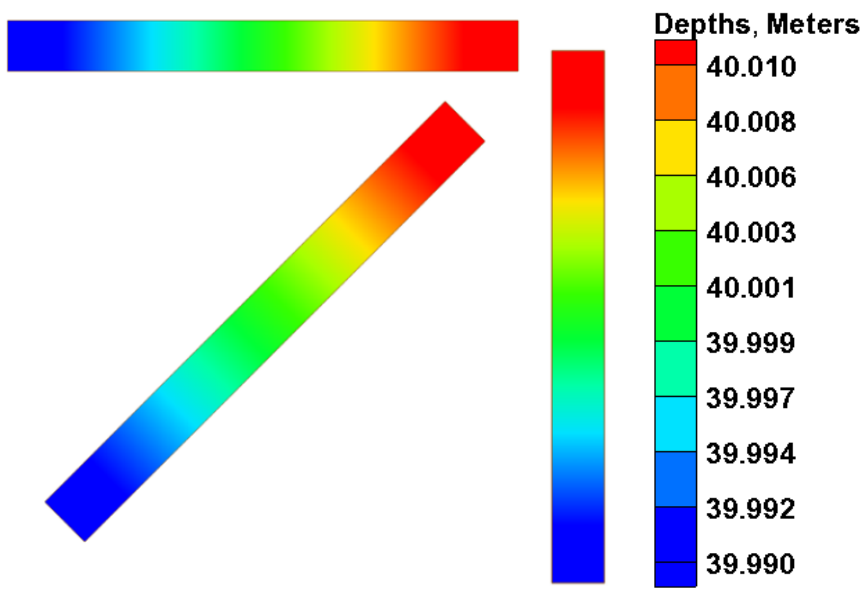

Figure 19: Depths for the three flume orientations with a constant wind shear of 0.1 N/m^2 .

The AdH velocity solution for the x-direction oriented flume for wind shears of 0.1 $\frac{N}{m^2}$ and 0.5 $\frac{N}{m^2}$ are provided in Figures 20 and 21.

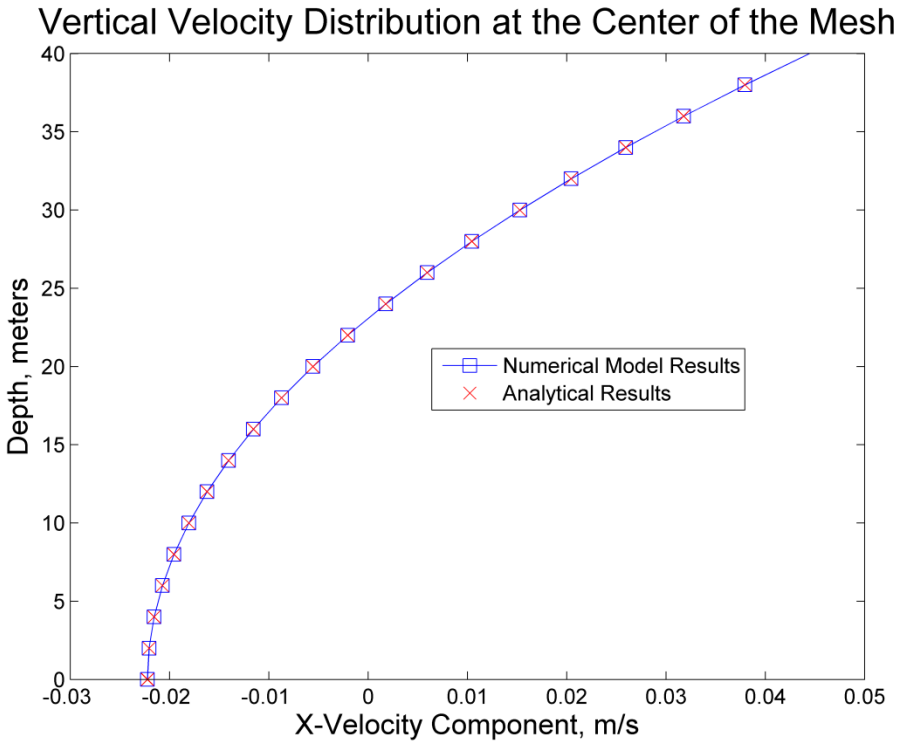

Figure 20: Velocity comparisons with a constant wind shear of 0.1 N/m^2 .

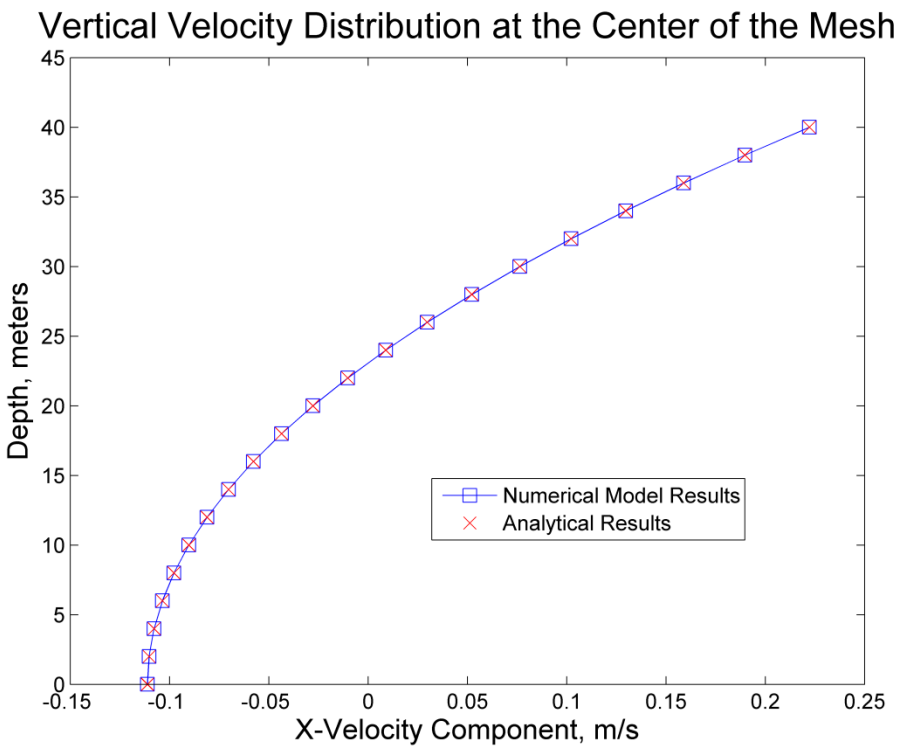

Figure 21: Velocity comparisons with a constant wind shear of 0.5 N/m^2 .

Comparisons of the model results and the analytical head differences and velocity results for all simulated configurations are provided in Table 10.

It should also be noted that the provided results were simulated on the SGI Altix ICE 8200 (Diamond) high performance computer (HPC). The simulations were performed on 8 processors. The simulation time ranged from approximately 13 minutes for the lowest resolution case to approximately 1.5 hours for the higher resolution cases. Several of the scenarios were also simulated on a personal computer (PC). The model solutions for both the HPC and PC computers produced equivalent results but the PC simulations required approximately 5 to 10 times longer to reach completion.

Table 10: Comparison of the AdH model results to the analytical solution for all simulated scenarios.

Horizontal Node Spacing (m)	Number of Vertical Layers	Wind Shear Applied (N/m^2)	Flume Orientation	Velocity - Root Mean Square Error (m/s)	Model Water Level Difference (m)	Analytical Water Level Difference (m)	Error in Model Water Level Difference (m)
500	20	0.1	X – Direction	2.0×10^{-6}	0.02545	0.02547	1.4×10^{-5}
500	20	0.1	Y – Direction	2.0×10^{-6}	0.02545	0.02547	1.4×10^{-5}
500	20	0.1	45 Degrees from X - Axis	2.0×10^{-6}	0.02545	0.02547	1.4×10^{-5}
500	20	0.5	X – Direction	3.0×10^{-5}	0.12754	0.12733	2.1×10^{-4}
500	20	0.5	Y – Direction	3.0×10^{-5}	0.12754	0.12733	2.1×10^{-4}
500	20	0.5	45 Degrees from X - Axis	3.0×10^{-5}	0.12754	0.12733	2.1×10^{-4}
500	12	0.1	X – Direction	5.4×10^{-5}	0.02545	0.02547	1.8×10^{-5}
500	8	0.1	X – Direction	1.7×10^{-4}	0.02544	0.02547	3.0×10^{-5}
500	6	0.1	X – Direction	2.9×10^{-4}	0.02542	0.02547	4.1×10^{-5}
500	3	0.1	X – Direction	6.4×10^{-4}	0.02602	0.02547	5.6×10^{-4}
1,000	20	0.1	X – Direction	4.5×10^{-5}	0.02538	0.02547	8.3×10^{-5}
2,000	20	0.1	X – Direction	8.2×10^{-4}	0.02537	0.02547	9.3×10^{-5}

Flow around an Emergent Spur Dike: Test of Turbulence Closure

This test, based upon the work presented in *Rajaratnam and Nwachukwu* (1983), is designed to test the accuracy and adequacy of the turbulence closure schemes implemented into the model. The schemes currently implemented in the model are the 2nd order Mellor Yamada (*1982)* in the vertical and Smagorinski (*1963*) in the horizontal.

The test domain is illustrated in figure 22. An emergent spur of 0.152 m length and 0.03 m width is placed 14.0 m downstream of the inflow location (at the left boundary). A uniform flow of 0.0453 m^3/sec and a tail water of 0.189 m are applied as the left and right boundaries respectively.

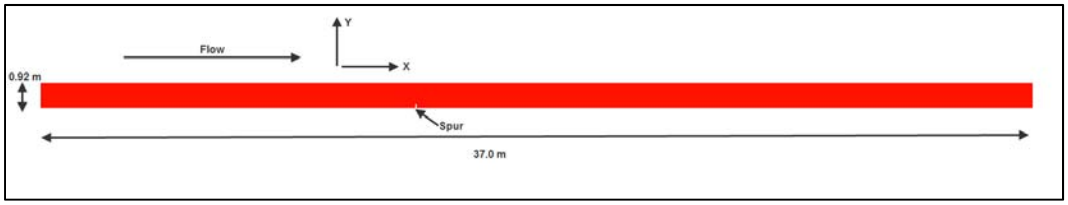

Figure 22: Domain for spur dike test.

The model parameters utilized are as follows:

Smagorinski coefficient: 0.2
Uniform background eddy viscosity: 0.0015 m^2/sec
Mannings 'n' value: 0.01.

Figure 23 shows the model computed recirculation at steady flow. The model computed a reattachment length of 11.8 times the spur length.

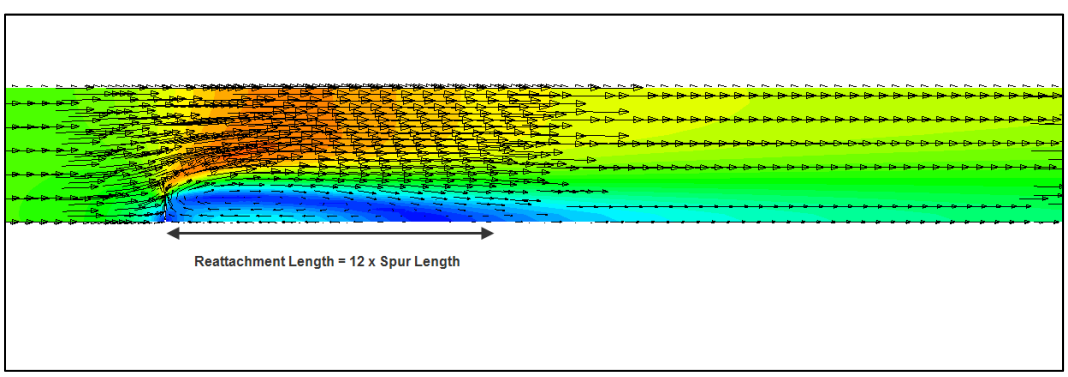

Figure 23: Model Computed Recirculation Zone

This value matches closely to the value of 12 times the spur length reported in literature (*Wang, et al, 2009*). Figure 24, illustrates the recirculation zone in the 'z' or the vertical plane.

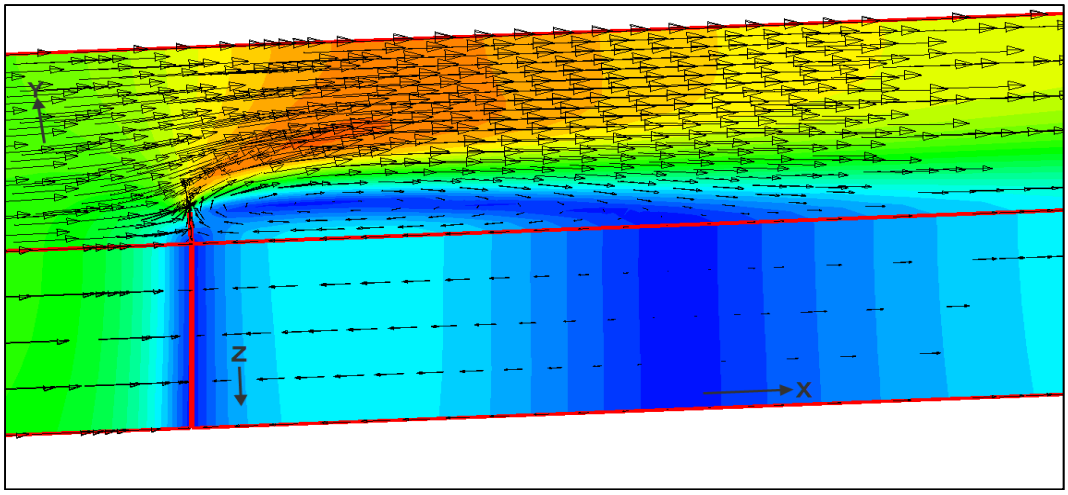

Figure 24: Model computed recirculation zone in the vertical or 'z' axis.

Horizontal Node Spacing (m)	Number of Vertical Layers	Total/Max Number of Nodes	Re-attachment Length (x Spur Length)	Average Velocity (m/sec)
0.1x0.1	4	31500	11.83	0.2568
0.05x0.05	8	219195	11.95	0.2571
0.1x0.1 (adaption)	4	31734	11.89	0.2569

Table 11: Simulation Results for Flow around a Spur Dike Test Case, 96 Compute Nodes

Propagation of Salinity Subsequent to a Lock Exchange

This test was run to ascertain the ability of the model to accurately represent the shock speed of a density wedge. The test consisted of a 2 m (long), 0.2 m (wide) and 0.2 m (deep) flume with denser salt water, 35 ppt, in the left half and freshwater , 0 ppt, in the right half. The barrier separating the two is instantaneously removed causing the denser fluid to slump under the lighter fluid and move as a density wedge. Figure 25 and 26 illustrate the domain and initial constituent state, respectively, for this test.

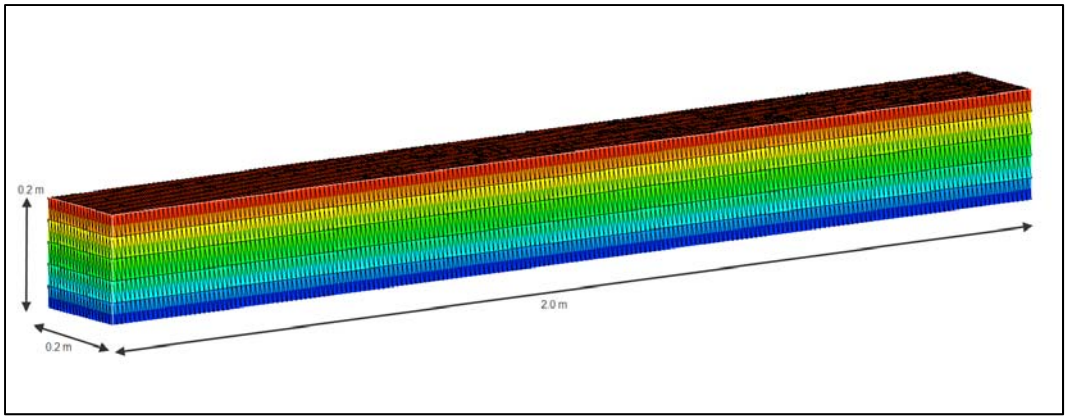

Figure 25: Domain for lock exchange

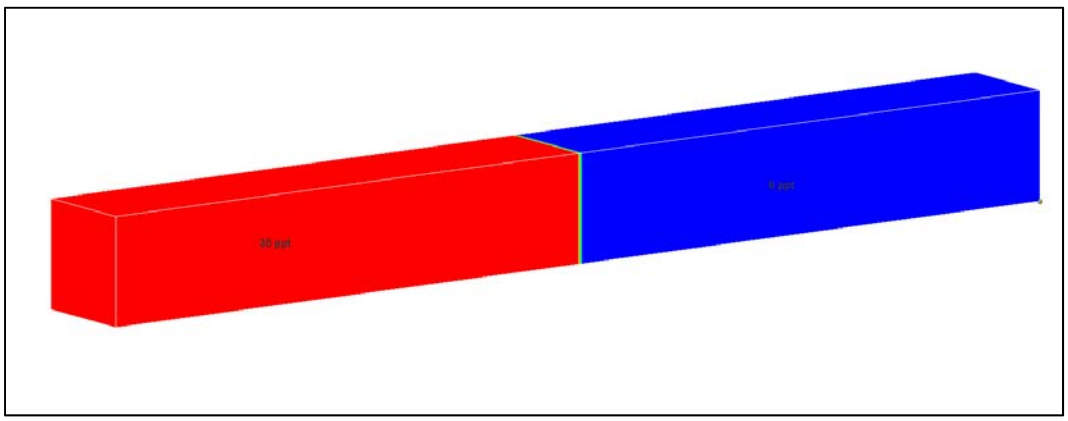

Figure 26: Initial Constituent state for lock exchange

The model computed shock speed in terms of the Froude number, represented as,

$$Fh = \frac{U}{\sqrt{g(1-\gamma)h}}$$

Where, U is the shock speed, γ is the ratio of lower density to higher density (0.997 for this test) , h is the total dense fluid depth. The 'Fh' computed for this test case is 0.5, this value is close to the reported value of 0.35 to 0.5 (*Shin et.al, 2004*) , 0.5 is the energy conserving value of non-rigid lid density currents. Figure 27 illustrates state of the model at 16 seconds from lock removal.

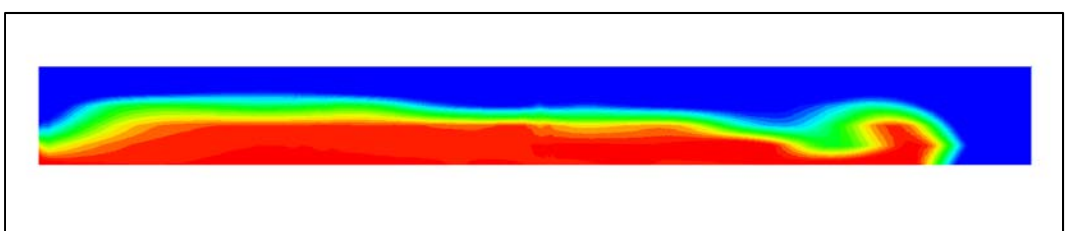

Figure 27: Base Case Constituent State at 16 seconds, red represents denser fluid.

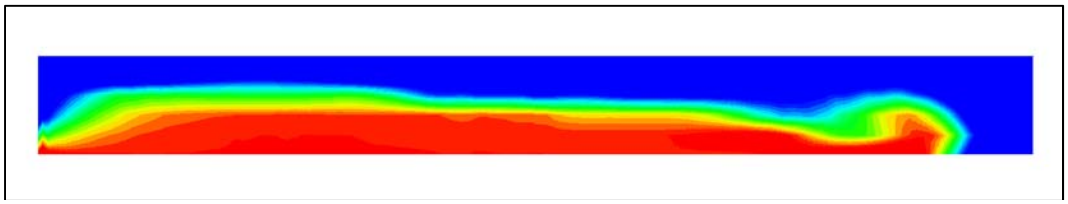

Figure 28: Base Case (with Adaption) Constituent State at 16 seconds, red represents denser fluid.

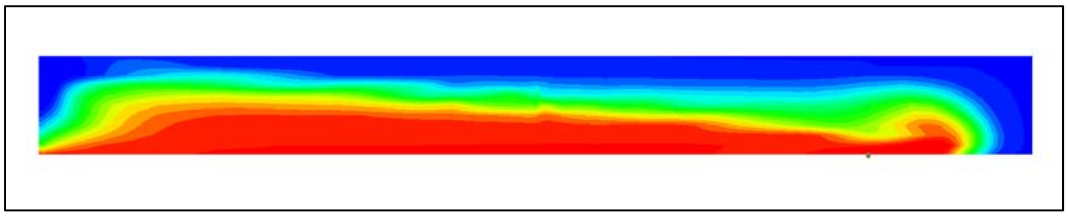

Figure 29: Twice Refined Mesh Case Constituent State at 16 seconds, red represents denser fluid.

Parameter	Base Mesh	Adapted Mesh	Twice Refined Mesh
Background Kinematic Eddy Viscosity	1E-07	1E-07	1E-07
Manning's "n"	0.03	0.03	0.03
Smagorinski Coefficient	0.2	0.2	0.2

Table 12: Simulation Parameters for Lock Exchange Test Case

Horizontal Node Spacing (m)	Number of Vertical Layers	Total/Max Number of Nodes	Froude Number
0.1x0.1	5	25326	0.50
0.05x0.05	10	180851	0.67
0.1x0.1 (adaption)	5	45819	0.53

Table 13: Simulation Results for Lock Exchange Test Case, 32 Compute Nodes

Horizontal Node Spacing (m)	Number of Vertical Layers	Total/Max Number of Nodes	Froude Number
0.1x0.1	5	25326	0.51
0.05x0.05	10	180851	0.65
0.1x0.1 (adaption)	5	45853	0.54

Table 14: Simulation Results for Lock Exchange Test Case, 96 Compute Nodes

Note that results from simulations on different number of processors are qualitatively and quantitatively similar.

Baroclinic Transport in Reservoir

This test case applied the model to the study of a temperature generated bottom density current. The test setup consisted of the *Generalized Reservoir Hydrodynamics (GRH)* described in Johnson (*1981)*. The primary purpose of this test was to "ascertain ability of the model to adequately and efficiently model a real problem that commonly occurs in reservoirs" (*Johnson, 1981).* Figures 30 and 31 illustrate the plan and side view of the modelled flume respectively.

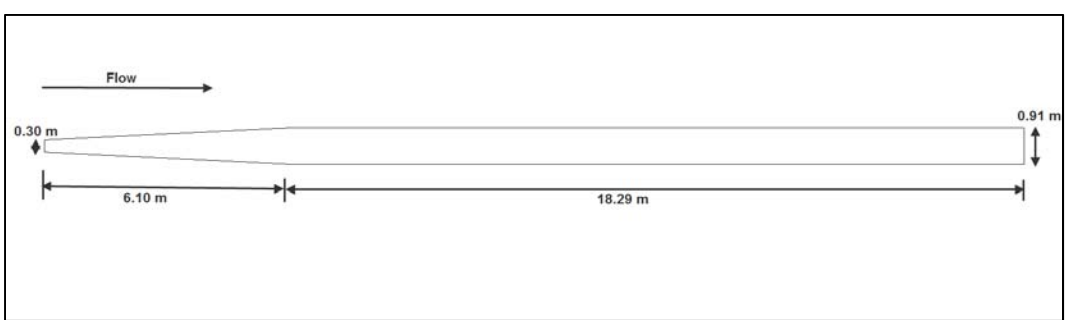

Figure 30: Plan View of GRH Test

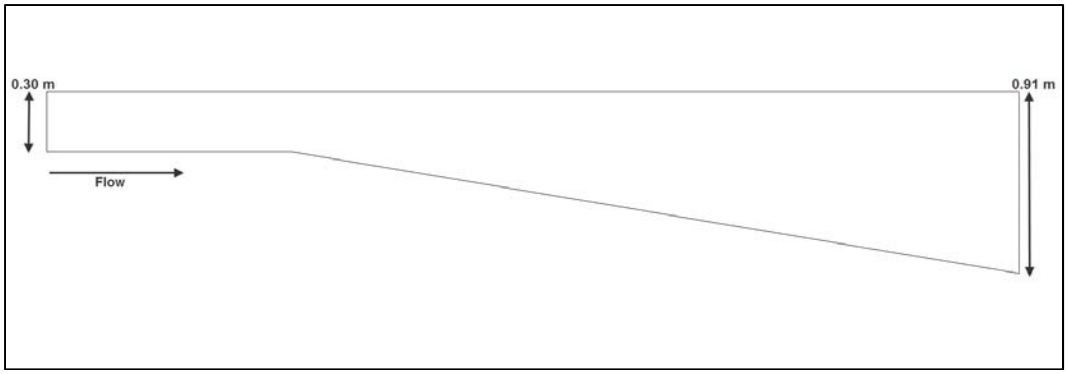

Figure 31: Side View of GRH Test

The inflow is specified at 0.00063 m^3/sec with a temperature of 16.7 ^oC, and is introduced into the flume over the bottom 0.15m of the upstream end. The outflow was extracted from a port situated at 0.15m from the bottom with a size of 0.0245m. The ambient temperature in the flume at test initialization was set at 21.4 ^oC. Observation show that the underflow generated takes between 17-18 minutes to reach the reservoir wall.

Table 15 lists the parameters utilized for this test application.

Parameter	Base Mesh	Adapted Mesh	Twice Refined Mesh
Background Kinematic Eddy Viscosity	1E-09	1E-09	1E-09
Manning's "n"	0.005	0.005	0.005
Smagorinski Coefficient	0.	0.	0.

Table 15: Simulation Parameters for GRH Test Case

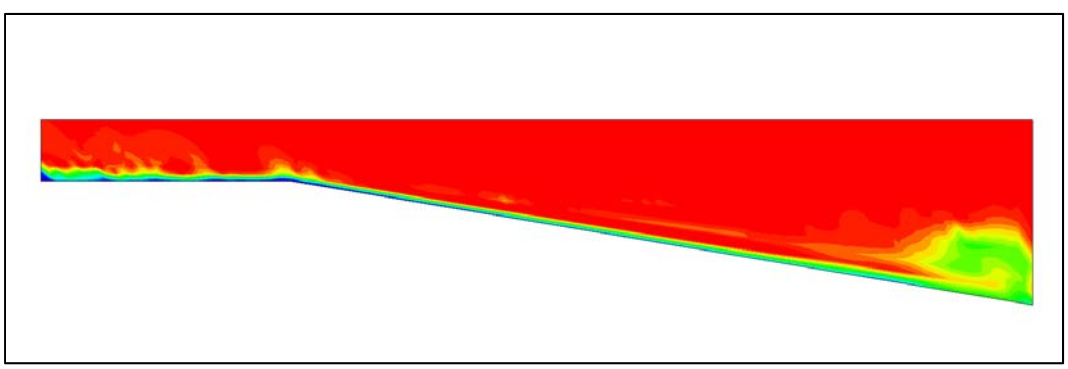

Figure 32: Base Model Simulated Underflow State at 1140 sec (19 min).

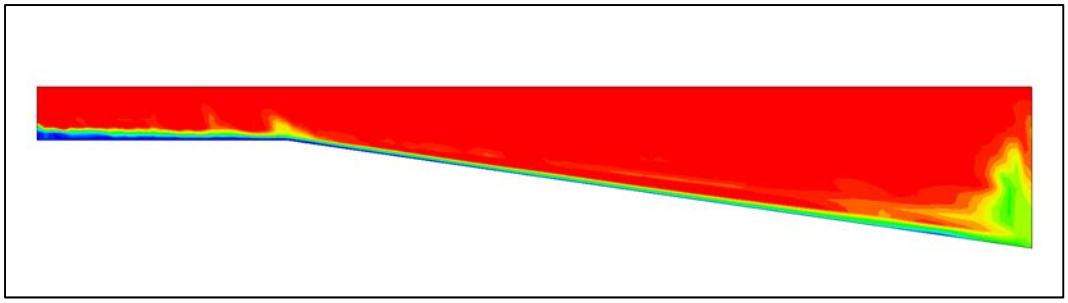

Figure 33: Twice Refined Model Simulated Underflow State at 1080 sec (18 min)

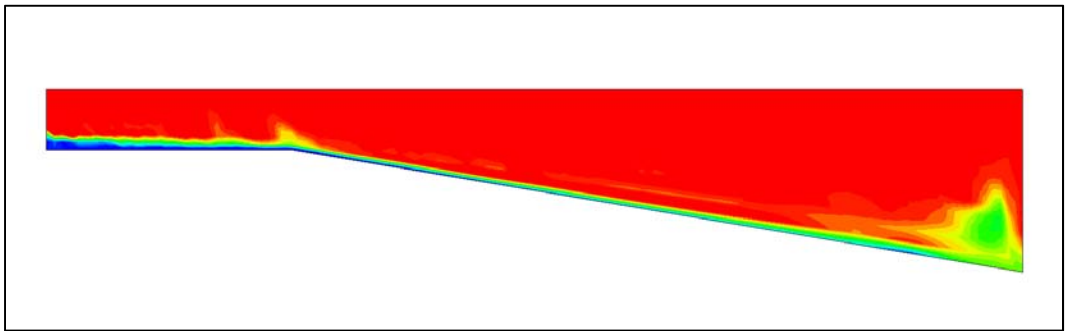

Figure 34: Adapted Base Model Simulated Underflow State at 1080 sec (18 min).

Figure 32 illustrates the model state at 19 minutes (base model), it is observed that the model simulated time required for the underflow to reach the reservoir wall closely matches that observed in the flume.

Figures 33 and 34 illustrate the twice refined model and the adapted base grid states at 18 minutes, it is observed that with additional refinement the underflow reaches the reservoir wall at approximately the same time as the physical observations.

Table 16 tabulates the results from the simulations performed for mesh convergence; note that the twice refined mesh provides the closest quantitative results to the observation but takes approximately twice as long as the adapted mesh which provides similar results.

Horizontal Node Spacing (m)	Number of Vertical Layers	Total/Max Number of Nodes	Model Time to Reservoir Wall (seconds)	Observed Time to Reservoir Wall (seconds)	Error (seconds)	Time to Completion (seconds)
0.2x0.1	8-14	17759	1140	1080	60	249
0.1x0.05	16-21	69400	1074	1080	-6	915
0.2x0.1 (adaption)	8-14	23510	1088	1080	8	463

Table 16: Simulation Results for GRH Test Meshes

3 Summary and Conclusions

This report lays out the verification and validation of the ADH-SW3 numerical hydrodynamics and baroclinic transport code.

The code was subjected to a series of analytic and flume tests to ascertain model capability to reproduce results with adequate accuracy. The tests executed included cases designed to test mass conservation, turbulence closure, wind stresses as well as model capability to model sharp baroclinic gradients across an interface.

As a result of these tests it has been proved that the ADH-SW3 code is capable of reproducing pertinent hydrodynamic and transport processes.

4 References

Johnson, B. H (1981). “A Review of Numerical Reservoir Hydrodynamic Modeling”, U.S. Army Engineer Waterways Experiment Station, Technical Report E-81-2, February 1981.

Mellor, G. L and Yamada, Tetsuji (1982). “Development of a Turbulence Closure Model for Geophysical Fluid Problems”, Reviews of Geophysics and Space Science, Vol. 20, No. 4, pp 851-875.

Shin, J.O.; Dalziel, S.B and Linden, P.F. (2004). “Gravity Currents Produced by Lock Exchange”, Journal of Fluid Mechanics, vol 521, pp 1-34.

Smagorinsky, J. (1963). “General Circulation experiments with the primitive equations I. The basic experiment”. Monthly Weather Review, vol 91, No. 3, pp 99-164.

Taylor, C and Davis, J (1975). “Tidal and Long Wave Propagation”, Elsevier, pp 111.

Wang, S. S. Y, Jia, Y, Roche, P.J, Smith, P.E and Schmalz, R.A (2009). “Verification and Validation of 3D Free Surface Flow Models”, American Society of Civil Engineering.